

MODELLING THE THERMO-ELASTIC PROPERTIES OF SKEWED WOVEN FABRIC REINFORCED COMPOSITES

E.A.D. Lamers, S.Wijskamp & R. Akkerman
Composites Group, Department of Mechanical Engineering, University of Twente,
The Netherlands

Keywords: composites, woven fabrics, thermo-elastic properties, warpage.

ABSTRACT

Woven fabrics prove to be a very convenient fibre reinforcement when prepreg layers have to be draped on to double curvature moulds. The process of draping causes the angle between the warp and weft yarns to vary over the product with this double curvature. As a result, the thermomechanical properties of the fibre reinforced composite material show a corresponding distribution. These thermo-elastic properties must be known in order to predict the shrinkage and warpage of the product.

Normally, composites consist of multiple fabric layers. These layers are oriented and skewed differently, and each contributes to the overall composite properties. Therefore, in order to predict the overall thermo-elastic properties of the composite as a whole, the properties of each individual layer must be known. In this paper, the inplane thermo-elastic properties of a woven fabric reinforced composite with an arbitrary weave type are analysed as a function of the skew angle, using micromechanics.

Three different levels of material structure are modelled, the micro-, the meso- and the macro level. The inplane thermo-elastic properties of four different basic elements are determined at the micro level, using geometrical shape functions and a two-dimensional thermo-elastic model. The inplane properties of one fabric layer are determined at the meso level, using the fabric pattern and the properties of the basic elements. At the macro level the homogeneous properties and warpage of woven fabric composites are considered. Here the composite structure and the properties of the individual layer are used.

The method proves to be a convenient way to model the skew deformation of the woven fabric composite and the resulting variation in the thermo-elastic properties. The theoretical predictions are verified by experiments on multiple-layered satin 5H woven fabric composites.

INTRODUCTION

Woven textile structures are often used as reinforcement in composite materials. Their ease of handling, low fabrication cost, good stability, balanced properties, and excellent formability make the use of woven fabrics very attractive for structural applications in, for example, the automotive and aerospace industry. However, due to the process of draping the fibre orientation varies over the product. During production these inhomogeneous properties will lead to internal stresses, which lead to product distortions, such as shrinkage and warpage.

Several models have been developed to predict the inplane thermo-elastic properties for various fabric weaves. Ishikawa and Chou (1,2) developed three one dimensional models for various types of orthogonal woven fabric composites; the mosaic model, the crimp model, and the bridging model. The two dimensional model of Naik and Shembekar (3,4) describes the full geometry of plain weave fabric laminates. The model predicts the inplane elastic properties in the load direction, based on the Classical Laminate Theory (5) and assuming a mixed parallel-series arrangement of infinitesimal pieces. Based on this model, Falzon and Herzberg (6) considered the effect of laminate configuration on the strength and stiffness properties. Vandeurzen and Verpoest (7,8) developed a Microsoft Excel® application, TEXCOMP, that describes the three dimensional geometry of various fabric weaves. Based on this geometry, they developed a model that predicts the three dimensional elastic properties of fabric composites. Akkerman and De Vries (9) developed a two-dimensional model for orthogonal fabric weaves. The model presented here is based on their work.

Here, the objective is to develop a model for the prediction of the inplane thermal and elastic properties of skewed woven-fabric composite laminates. The method is verified with thermomechanical tests on orthogonal and skewed 5H satin weave laminates.

MODELLING ORTHOGONAL FABRIC COMPOSITES

In order to predict the thermo-elastic properties of a fabric reinforced composite, three structural levels are distinguished: the macro-, the meso- and the micro-level. At the macro level, the homogeneous properties of the fabric composite are determined from the individual layer properties. The properties of the individual fabric layers are determined at the meso level. The meso level uses the properties found in the micro level, where the building blocks of the fabric are determined, based on a geometrical description of the weave.

Geometrical representation of the weave

In the weave (the geometrical structure of the fabric), two of the three structural levels are determined, the meso- and micro level. Repetitive units (called unit cells) are distinguished at the meso level. These unit cells are the smallest regions that still can represent the overall weave. They are found in any regular two-dimensional weave. Unit cells consist of fabric elements, which are characteristic for each weave type. The fabric elements are composed of basic elements. These basic elements are the building blocks for any two-dimensional fabric weave type. For each weave type, the unit cell and the fabric elements are different.

In **Fig 1**, an example of a unit cell is shown. The figure represents a 5H satin unit cell with most warp yarns on top. The unit cell, marked with the dotted line, is composed of twenty-five fabric elements. Three different types of fabric elements can be distinguished, each consisting of four basic elements. In **Fig 1**, some of the basic elements have a minus sign. The minus sign indicates that the fill yarn is on top.

In the basic elements regions of warp yarns, fill yarns and pure resin can be distinguished. The size of these regions determines the average fibre volume fraction in the yarn regions, when the overall fibre volume fraction is known. For each of these basic elements the interfaces between the regions are modelled by the geometrical shape functions of the yarns, similar to the work of Naik and Shembekar (3,4). The yarn shape functions are defined as the sum of two parts: the yarn midplane functions and the yarn cross-sectional shape functions. When taking the inplane contribution of each yarn and applying symmetry and rotation rules, four different basic cells are found.

The yarn midplane is the surface through the centre of gravity of the yarn and the inplane direction normal to the yarn. The yarn midplane can either be a plane surface or a curved surface. In **Table I**, the basic element types and their yarn midplanes are listed.

Microscopic investigations of the weave have demonstrated undulated parts of the yarns. The undulation factors U_w and U_f are used to model these undulated regions. Because the warp and fill yarns are on top of each other, the midplane and the cross sectional shape are directly related by the undulation factor. In **Fig 2**, the undulated length in a fill yarn is shown. The undulation factors are related to the undulated lengths by

$$L_{w,f} = U_{w,f} \cdot w \quad [1]$$

where $L_{w,f}$ is the undulated length and w is the width of the basic element. The resulting mathematical representations of the geometrical yarn midplanes are presented in **Table II**.

In the basic elements, the cross section for the warp and the fill yarns is assumed to be constant and homogeneous. Taking the undulating relations into account leads to the mathematical representations of the cross sections of the yarns as presented in **Table III**.

The shape functions of the basic elements, defining the interfaces between regions of pure resin and yarns (UD-composite), are created by a summation of the midplane functions and the cross-sectional yarn shape functions. When also defining the top and bottom plane and a middle surface, seven surfaces define all interfaces. The graphical representation of the basic elements using the geometrical shape functions is displayed in **Fig 4**.

Thermo-elastic modelling of orthogonal fabric

Using the geometrical representation of the weave, the thermo-elastic properties of the basic elements are calculated. With these properties, the properties of the fabric elements and the repetitive unit are determined. Finally, the thermo-mechanical properties of the entire composite can be modelled. In this analysis, a distinction is made between the mechanical and the thermal properties.

To determine the mechanical properties of the basic elements, it is assumed that the Classical Laminate Theory (CLT) is applicable to each of the basic elements. Therefore, the constitutive equation for the inplane mechanical properties for the basic elements is:

$$\begin{pmatrix} N_i \\ M_i \end{pmatrix} = \begin{bmatrix} A_{ij}(x,y) & B_{ij}(x,y) \\ B_{ij}(x,y) & D_{ij}(x,y) \end{bmatrix} \begin{pmatrix} \varepsilon_j^0 \\ \kappa_j \end{pmatrix} \quad (i,j = 1,2,6) \quad [2]$$

and

$$(A_{ij}(x, y), B_{ij}(x, y), D_{ij}(x, y)) = \int_{h_B^k}^{h_T^k} (1, z, z^2) Q_{ij} dz \quad [3]$$

in which Q_{ij} is the elastic inplane stiffness matrix (derived from the principal elastic constants (6)), z the height co-ordinate of the layer, h_B^k is the bottom co-ordinate of the fabric layer, and h_T^k is the top co-ordinate of the fabric layer. The effective inplane elastic constants of the warp and fill yarns can be described using the undulation angle of these yarns, while the elastic properties in the principal directions for UD yarn composites are calculated using the Composite Cylinder Assemblage (CCA) model (10,11). The resulting inplane stiffness matrices, using the boundaries defined by the shape functions are:

$$A_{ij}^e(x, y) = Q_{ij}^R [h_{w_t}^e(x, y) - h_t^e(x, y) + h_{F_t}^e(x, y) - h_{w_b}^e(x, y) + h_b^e(x, y) - h_{F_b}^e(x, y)] + Q_{ij}^W(\theta_x) [h_{w_b}^e(x, y) - h_{w_t}^e(x, y)] + Q_{ij}^F(\theta_y) [h_{F_b}^e(x, y) - h_{F_t}^e(x, y)]$$

$$B_{ij}^e(x, y) = Q_{ij}^R [h_{w_t}^e(x, y)^2 - h_t^e(x, y)^2 + h_{F_t}^e(x, y)^2 - h_{w_b}^e(x, y)^2 + h_b^e(x, y)^2 - h_{F_b}^e(x, y)^2] + Q_{ij}^W(\theta_x) [h_{w_b}^e(x, y)^2 - h_{w_t}^e(x, y)^2] + Q_{ij}^F(\theta_y) [h_{F_b}^e(x, y)^2 - h_{F_t}^e(x, y)^2] \quad [4]$$

$$D_{ij}^e(x, y) = Q_{ij}^R [h_{w_t}^e(x, y)^3 - h_t^e(x, y)^3 + h_{F_t}^e(x, y)^3 - h_{w_b}^e(x, y)^3 + h_b^e(x, y)^3 - h_{F_b}^e(x, y)^3] + Q_{ij}^W(\theta_x) [h_{w_b}^e(x, y)^3 - h_{w_t}^e(x, y)^3] + Q_{ij}^F(\theta_y) [h_{F_b}^e(x, y)^3 - h_{F_t}^e(x, y)^3]$$

where the superscript R , W and F denote resin, warp and fill, respectively, and superscript e denotes the type of basic element (A,B,C or D). The undulation angles θ_x and θ_y are defined as

$$\theta_x = \arctan\left(\frac{\partial h_{wSh}(x, y)}{\partial x}\right) \quad \theta_y = \arctan\left(\frac{\partial h_{FSh}(x, y)}{\partial y}\right) \quad [5]$$

Using the 2D WF model (3,4), the average inplane constants for each basic element can now be obtained. The model can predict two boundaries by assuming uniform inplane strain or stress conditions, respectively called the *Parallel-Parallel (PP)* configuration and the *Series-Series (SS)* configuration,

$$(\bar{A}_{ij}^{pp}, \bar{B}_{ij}^{pp}, \bar{D}_{ij}^{pp}) = \frac{4}{w^2} \int_0^{w/2} \int_0^{w/2} (A_{ij}^e(x, y), B_{ij}^e(x, y), D_{ij}^e(x, y)) dy dx \quad [6]$$

$$(\bar{a}_{ij}^{ss}, \bar{b}_{ij}^{ss}, \bar{d}_{ij}^{ss}) = \frac{4}{w^2} \int_0^{w/2} \int_0^{w/2} (a_{ij}^e(x, y), b_{ij}^e(x, y), d_{ij}^e(x, y)) dy dx \quad [7]$$

The integrals are evaluated numerically, using Gaussian quadrature.

The thermal properties of the basic elements are determined under the same assumptions as the mechanical properties of the basic elements. The constitutive equations for the thermal properties then become:

$$\begin{pmatrix} N_i \\ M_i \end{pmatrix} = -\Delta T \begin{pmatrix} \tilde{A}_i \\ \tilde{B}_i \end{pmatrix} \quad \text{in which} \quad \begin{pmatrix} \tilde{A}_i \\ \tilde{B}_i \end{pmatrix} = \int_{h_B^k}^{h_T^k} (1, z) q_i dz, \quad [8]$$

$$q_i = Q_{ij} \cdot \alpha_j(\theta)$$

where α_j for the warp and fill yarns depends on the fibre volume fraction and is determined using the model of Shapery (12). When assuming no external force the resulting thermal strain and curvature are:

$$\begin{pmatrix} \varepsilon_i^0 \\ \kappa_i \end{pmatrix} = \Delta T \cdot \begin{bmatrix} a_{ij} & b_{ij} \\ b_{ij}^T & d_{ij} \end{bmatrix} \cdot \begin{pmatrix} \tilde{A}_i \\ \tilde{B}_i \end{pmatrix} \quad [9]$$

This results in the inplane thermal expansion and bending coefficients $\tilde{\alpha}$ and $\tilde{\beta}$:

$$\begin{pmatrix} \tilde{\alpha}_i \\ \tilde{\beta}_i \end{pmatrix} = \begin{bmatrix} a_{ij} & b_{ij} \\ b_{ij}^T & d_{ij} \end{bmatrix} \cdot \begin{pmatrix} \tilde{A}_i \\ \tilde{B}_i \end{pmatrix} \quad [10]$$

The thermally induced forces and moments \tilde{A}_i and \tilde{B}_i are determined by substituting Q_{ij} by q_i in equation [4].

The thermo-elastic properties of the fabric elements and unit cell are determined by averaging the properties of the basic elements. Averaging again leads to the unit cell properties. Alternatively, a Finite Element approach can be used (9), leading to closer bounds. The unit cell properties are then used to determine the composite properties, taking into account the relative position of the fabric layer to the midplane of the composite. When h_0 is the distance of the midplane of the fabric layer to the midplane of the composite, the contribution of each individual layer is:

$$\begin{aligned} A_{ij}^C &= \sum_{k=1}^m A_{ij}^k \\ B_{ij}^C &= \sum_{k=1}^m h_0^k \cdot A_{ij}^k + B_{ij}^k \\ D_{ij}^C &= \sum_{k=1}^m h_0^{k^2} \cdot A_{ij}^k + 2 \cdot h_0^k \cdot B_{ij}^k + D_{ij}^k \end{aligned} \quad [11]$$

where C denotes composite and m is the number of fabric layers in the composite. The thermal properties of the composite are derived similarly to those of the individual layers.

MODELLING SKEWED FABRIC

In many applications, the fabric is neither orthogonal nor uniformly deformed. For the prediction of shrinkage and warpage the thermomechanical properties need to be defined as a function of the skew angle. Skewed means in this context a pure shear deformation of the weave, where the cross-over points in the weave act as pivoting points.

Geometrical representations of the skewed weave

In the analysis of the skewed weave, the same subdivision is made in unit cell, fabric elements and basic elements. It is not possible to determine the properties by transforming the matrices of orthogonal fabric directly. Instead, the geometry is transformed by a pure shear deformation, transforming the orthogonal axes into skewed axes, as depicted in **Fig 5**, or mathematically described by

$$\begin{pmatrix} x' \\ y' \end{pmatrix} = \begin{bmatrix} 1 & 0 \\ \cos(\varphi) & \sin(\varphi) \end{bmatrix} \cdot \begin{pmatrix} x \\ y \end{pmatrix} \quad [12]$$

where x' and y' are the transformed axes and φ the skew angle. As a result of this transformation, the yarn shape functions will transform according to:

$$h(x', y') = h(x, y) \quad [13]$$

The area of the unit cell decreases with increasing skew angle, resulting in an increase in the fibre volume fraction, when the layer thickness is assumed constant,

$$V_f(x, y) = V_f(x', y') \cdot \sin(\varphi) \quad [14]$$

Thermo-elastic modelling of skewed fabric

The thermo-elastic properties of the skewed fabric are determined in a similar way to the orthogonal fabric. For the basic elements, the effective inplane elastic constants of the warp and fill yarns are now described using the integration boundaries and the undulation angle in the (x', y') co-ordinate axes. The properties of the skewed fabric elements, skewed repetitive unit and the fabric composite are determined using the same methods as used before.

EXPERIMENTAL WORK

The thermoelastic properties of carbon fibre (Torayca T300 B) reinforced thermoplastic composites were measured in order to validate the model. The symmetrical test laminates were manufactured from 4-layers of satin 5H fabric (CD0285), in a semi-crystalline thermoplastic resin, Poly Phenylene Sulfide (PPS). The laminates were made by compression moulding in a closed mould of 250*250 mm, resulting in a fibre volume fraction 59% in orthogonal fabric composites. In **Table IV**, an overview of the material properties is displayed. Ten Cate Advanced Composites supplied both materials.

Tensile tests were performed using a Zwick type 1445 machine with a 10 kN load cell in a temperature and humidity controlled environment. The specimens were cut in the 0°, 45° and 90° direction with the major principal axis of the material. The load was directly obtained from the tensile testing machine, while the strain was measured by strain gauges. For the tensile tests, the specimens were prepared according to the ASTM D3039-76 protocol (13). The skew angles of the fabric were 0° for the orthogonal, 22° for the intermediate skew and 35° for the locked specimens. The results are presented in **Fig 6**, showing the properties in abhd-compliance matrix form. Measurements of the linear thermal expansion were performed on the orthogonal specimens only, as displayed in **Fig 7**.

RESULTS AND DISCUSSION

The effects of skew deformation on the thermo-elastic properties are illustrated by performing a simulation of tensile tests in the principal directions (**Fig 8**). This results in a significant increase of the apparent modulus in the 1-direction due to the fibre reorientation. In the 2-direction little decrease is observed, as the decrease due to the fibre reorientation is compensated by the increase in fibre volume fraction.

The results from tensile tests, performed on orthogonal fabric, show good agreement with the modelled values when using the *PP*- configuration. The experimental results for the a_{66} property display a large scatter. In spite of this scatter, the model, even with the *PP*- configuration underestimates the experimental value. This phenomenon is not explained and requires further investigation.

In modelling the experimental properties obtained from the tensile test performed on the skewed fabric, the model reasonably predicts the values. The model gives good results in the major principal direction (a_{11}). Perpendicular to this direction (a_{22}), the experimental values

are underestimated. This can be explained by the larger relative contribution of the inplane shear stiffness in the direction.

The experimental coefficient of linear thermal expansion (CTE), measured on orthogonal fabric, is predicted nicely by the *PP*-configuration. The *SS*-configuration overestimates the linear thermal expansion, corresponding to the overestimation of the inplane compliance.

CONCLUSION

A model was presented to determine the inplane thermo-elastic properties of woven fabric laminates. It gives a reasonable correlation with the experimental results for a 5H satin fabric when a uniform state of basic element strain is used (upper bound for the stiffness). In case a uniform state of basic element stress is assumed (lower bound for the stiffness), the laminate stiffnesses are underestimated. The bounds for the uniform strain and stress are quite far apart. The use of a FE formulation should result in closer bounds for the thermo-elastic properties of woven fabric laminates. Research is continued on the development of this FE formulation.

TABLES

Basic element	A	B	C	D
Warp midplane	Curved surface	Plane surface	Plane surface	Curved surface
Fill midplane	Curved surface	Plane surface	Curved surface	Plane surface

Table I: Basic elements and their midplane

Midplane	Geometrical shape function
Plane surface	$h_{WPTr,FPTr}(x, y) = \zeta \left(\frac{h_{tot}}{6} + \frac{h_{fib}}{12} \right)$
Curved surface	$\text{if } \xi < w.(1 - U_{w,f}) \quad h_{WCtr,FCtr}(x, y) = \zeta \left(\frac{h_{tot}}{6} + \frac{h_{fib}}{12} \right)$ $\text{if } \xi \geq w.(1 - U_{w,f}) \quad h_{WCtr,FCtr}(x, y) = \zeta \left(\frac{h_{fib}}{4} \cdot \cos \left(\frac{(\xi - w + w.U_{w,f})\pi}{2.w.U_{w,f}} \right) + \frac{(h_{tot} - h_{fib})}{6} \right)$
where $\xi = x$ and $\zeta = 1$ for warp midplane while $\xi = y$ and $\zeta = -1$ for fill midplane	

Table II: Yarn midplane

	Geometrical shape function
Yarn shape	$\text{if } \xi < w.(1 - U_{f,w}) \quad h_{WSh,FSH}(x, y) = \frac{h_{fib}}{4}$ $\text{if } \xi \geq w.(1 - U_{f,w}) \quad h_{WSh,FSH}(x, y) = \frac{h_{fib}}{4} \cdot \cos \left(\frac{(\xi - w + w.U_{f,w})\pi}{2.w.U_{f,w}} \right)$
where $\xi = y$ for warp midplane while $\xi = x$ for fill midplane	

Table III: Yarn shape functions

Material property	Unit	Carbon	PPS

Longitudinal modulus	[GPa]	231 [#]	3.70 [#]
Transverse modulus	[GPa]	14 [*]	3.70 [#]
Inplane Shear modulus	[GPa]	9 [*]	1.35 [#]
Transverse Shear Modulus	[GPa]	4 [*]	1.35 [#]
Inplane Poisson ratio		0.2 [*]	0.37 [#]
Longitudinal linear thermal expansion coefficient	[1/K]	-7E-7 [*]	51e-6 [#]
Transverse linear thermal expansion coefficient	[1/K]	5.6E-6 [*]	51e-6 [#]
Density	[kg/m ³]	1750 [#]	1350 [#]

Table IV: Material properties of carbon fibres and PPS resin

* values were obtained from literature [14].

values were obtained from manufacturer.

FIGURES

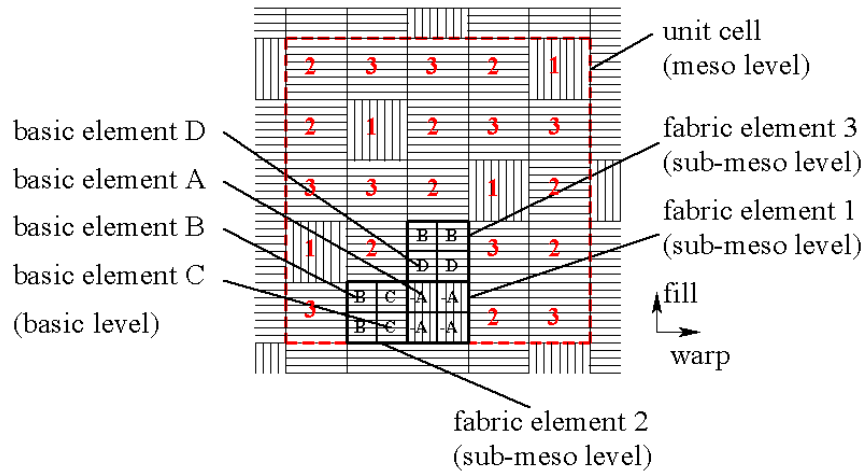


Fig 1: Unit cell of Satin 5H weave, with fabric elements 1, 2, 3 and basic elements A,B,C,D

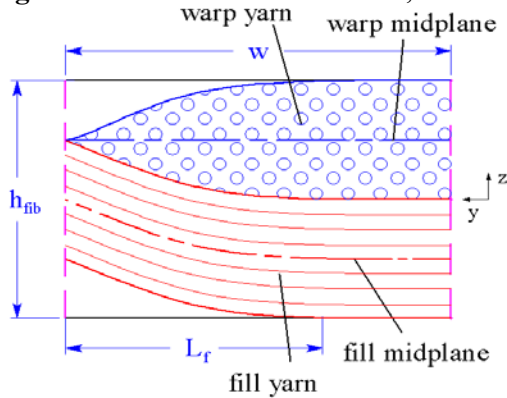


Fig 2: Undulated length of fill yarn midplane

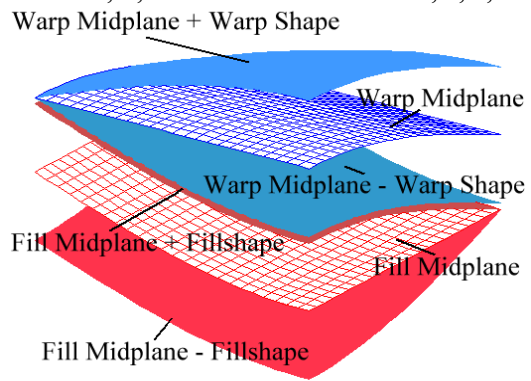


Fig 3: Construction of yarn functions

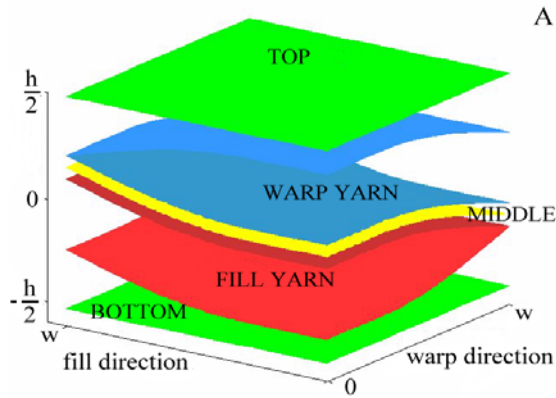


Fig 4^a: Basic element A

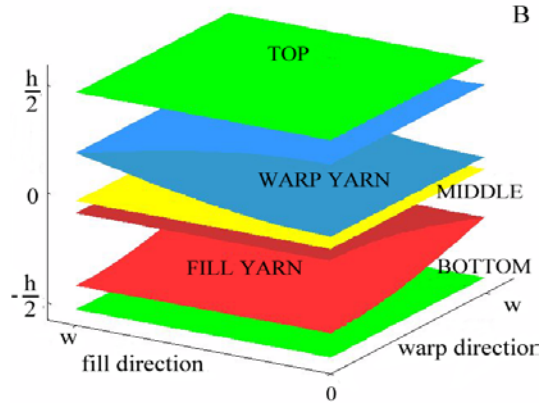


Fig 4^b: Basic element B

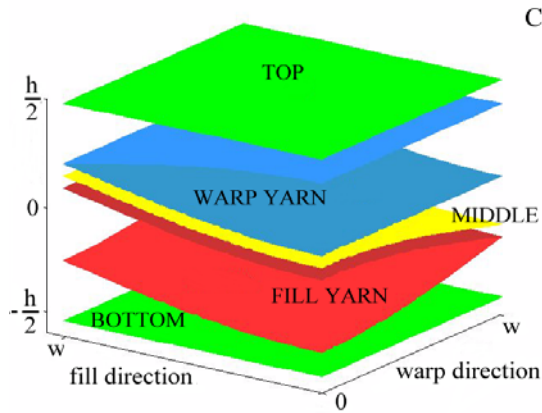


Fig 4^c: Basic element C

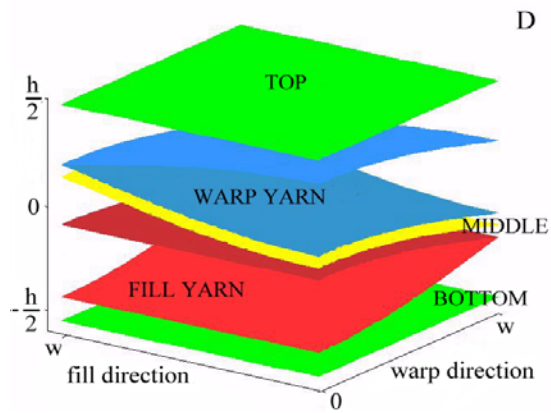


Fig 4^d: Basic element D

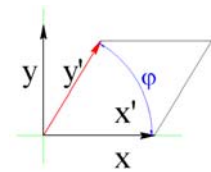


Fig 5: Transformation of axes

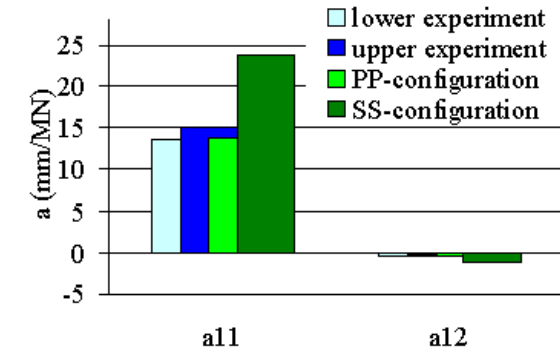


Fig 6^a: Orthogonal results (a_{11} and a_{12})

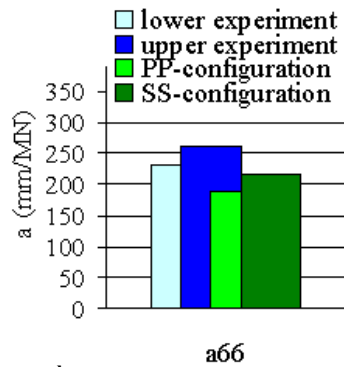


Fig 6^b: Orthogonal results (a_{66})

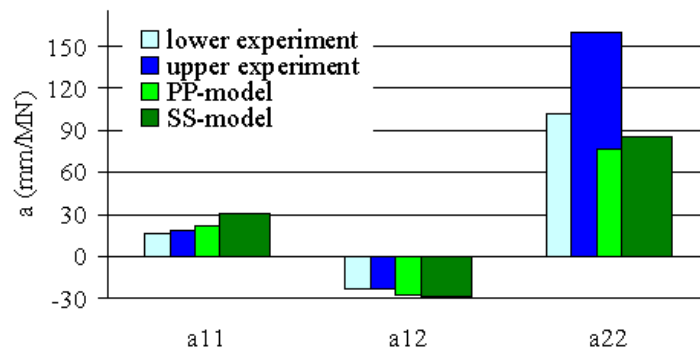


Fig 6^c: Intermediate skew fabric results (a_{11} , a_{12} and a_{66})

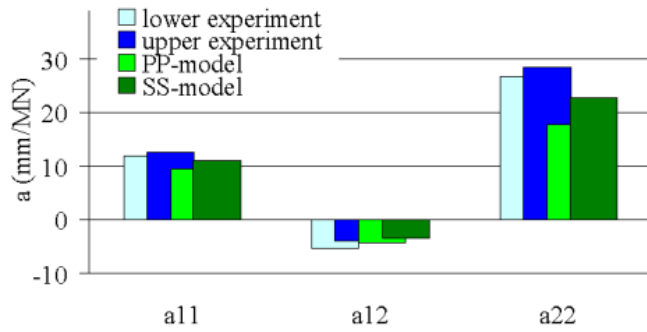


Fig 6^d: Locked fabric results (a₁₁, a₁₂ and a₆₆)

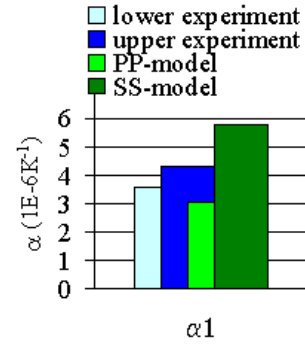


Fig 7: CTE for orthogonal fabric

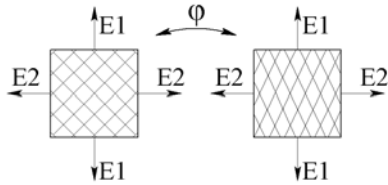


Fig 8: Loading of fabric

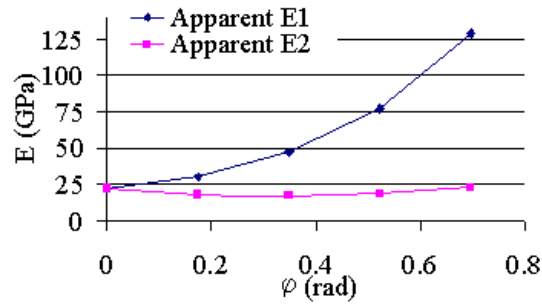


Fig 9: Apparent moduli of skewed fabric

LIST OF SYMBOLS

$h_{tot, fib}$	total lamina, dry fabric thickness (m)
$U_{w,f}$	warp, fill undulation factor
$L_{w,f}$	warp, fill undulation length (m)
w	width of half the (orthogonal) fabric element (m)
N_i, M_i	Force (N), Moment (N.m), with $i = 1,2,6$
$\varepsilon_j^0, \kappa_j$	midplane strain, curvature of fabric layer (m ⁻¹), $j = 1,2,6$
A_{ij}, B_{ij}, D_{ij}	inplane stiffness matrix (N.m ⁻¹ , N, N.m)
a_{ij}, b_{ij}, d_{ij}	inplane compliance matrix (N ⁻¹ .m, N ⁻¹ , (N.m) ⁻¹)
φ	skew angle (rad)
$\theta_{x,y}$	undulation angle (rad)
V_f	Fibre volume Fraction
$\tilde{\alpha}, \tilde{\beta}$	Inplane thermal expansion and bending coefficients (K ⁻¹ , (K.m) ⁻¹)
α	thermal expansion coefficient of fibres (K ⁻¹)

REFERENCES

1. Chou T W, Ishikawa T, Textile Structural Composites (1991), 31-37.
2. Chou T W, Ishikawa T, Textile Structural Composites (1991), 209-264.
3. Naik N K, Shembekar P S, J. of Composite Materials 26 (1992), 2196-2225.
4. Naik N K, Shembekar P S, J. of Composite Materials 26 (1992), 2227-2246.
5. Powell P C, 'Engineering with Fibre-Polymer Laminates', Chapman & Hall, 1994.
6. Falzon P F, Herzberg I, J. of Composite Materials 30 (1996), 1211-1247.
7. Vandeurzen P, Ivens J, Verpoest I, Composites Science and Technology 56 (1996), 1303-1315.

-
8. Vandeurzen P, Ivens J, Verpoest I, Composites Science and Technology *56* (1996), 1317-1327.
 9. Akkerman R, De Vries R S, in: Gibson A.G. (editor), International Conference on Fibre Reinforced Composites FRC'98 (1998), 422-433.
 10. Hashin, Z., J. of Applied Mechanics (1983), 50:481.
 11. Hashin, Z., *Theory of Fibre Reinforced Materials*, NASA-CR (1972).
 12. Schapery R A, J. of Composite Materials *2* (1975), 380-404.
 13. ASTM D 3039-76, Annual book of ASTM Standards Vol 08.01 (1989).
 14. Gibson R F, 'Principles of Composite Material Mechanics', McGraw-Hill, 1994.